Characterization of genes involved in ceramide metabolism in the Pacific oyster (*Crassostrea gigas*)

Emma Timmins-Schiffman[1] and Steven Roberts*[1]

[1]University of Washington
School of Aquatic and Fishery Sciences
Seattle, WA 98105

*Correspondence to: Steven Roberts
University of Washington
School of Aquatic and Fishery Sciences
Box 355020
Seattle, WA 98195-5020
sr320@uw.edu
(206) 685-3742 (phone)

ABSTRACT

Ceramide is a key component of the vertebrate stress response, however, there is limited information concerning its role in invertebrate species. In order to identify genes involved in ceramide metabolism in bivalve molluscs, Pacific oyster genomic resources were examined for genes associated with ceramide metabolism and signaling. Several genes were identified including full-length sequences characterized for *serine palmitoyltransferase-1*, *3-ketodihydrosphingosine reductase, acid ceramidase*, and *ceramide glucosyltransferase*. Genes involved in ceramide synthesis and metabolism are conserved across taxa in both form and function. Expression analysis as assessed by quantitative PCR indicated all genes were expressed at high levels in the gill tissue. The role of the ceramide pathway genes in the invertebrate stress response was also explored by measuring expression levels in juvenile oysters exposed to *Vibrio vulnificus*. A gene involved in hydrolytic breakdown of ceramide, *acid ceramidase*, was upregulated in a bacterial challenge, suggesting a possible role of ceramide in the invertebrate stress and immune responses.

KEYWORDS: oyster; *Crassostrea gigas*; ceramide; stress; *Vibrio*; immune; gene discovery; mollusc

INTRODUCTION

Ceramide is a sphingolipid that serves as an important signaling molecule for a variety of cellular processes including differentiation, proliferation, inflammation, and apoptosis (reviewed in Hannun 1994 and Ballou et al. 1996). Different stimuli promote either *de novo* synthesis of ceramide or its catabolic generation from sphingolipids (Hannun 1994; Ballou et al. 1996). The diversity of processes in which ceramide plays a role as a signaling molecule indicates its importance across a variety of life stages and environmental conditions. For example, the accumulation of ceramide can halt embryonic development (Eliyahu 2007), inhibit insulin signaling (Chavez et al. 2005), and promote apoptosis during cellular stress (Perry et al. 2000). The production of ceramide can be triggered by multiple pathways and is sensitive to exogenous stressors (Strelow et al. 2000; Perry et al. 2000). In sea bass (*Diecentrarchus labrax*), changes in intracellular ceramide levels in gill tissue are associated with abrupt shifts in environmental salinity (El Babili et al. 1996). Leukemia cells exposed to various exogenous stressors (ionizing radiation, hydrogen peroxide, UV radiation, and heat shock) showed elevated levels of ceramide and increased apoptosis (Verheij et al. 1996).

Ceramide metabolism has also been associated with immune-related processes. Cytokines can trigger sphingomyelin hydrolysis, leading to increased production of ceramide, suggesting that ceramide could propagate cytokine signaling (Ballou et al. 1996). Ceramide also plays a key role in the inflammatory response in *H. sapiens* dermal fibroblasts by stimulating interleukin-1 mediated prostaglandin E2 production (Ballou et al. 1992).

While the role of ceramide as a signaling molecule in response to stress has been well studied in mammalian systems, there is little information regarding the function and metabolism of ceramide in invertebrates. Given the range of environmental conditions experienced by intertidal species, ceramide signaling could be a key component in the cellular response to these environmental changes. The primary goal of this study was to characterize genes associated with ceramide metabolism in the intertidal mollusc, the Pacific oyster (*Crassotrea gigas*). Using an *in silico* approach, numerous genes associated with ceramide metabolism were identified and complete coding sequences were isolated for select genes. To provide insight into the functional role of ceramide metabolism in the invertebrate stress response, juvenile *C. gigas* were exposed to the marine bacterium *Vibrio vulnificus* and the expression levels of four genes involved in the ceramide pathway were assessed.

MATERIALS AND METHODS

Gene discovery

Genes involved in *C. gigas* ceramide metabolism were identified using publicly available sequence data. Specifically, short read sequences from *C. gigas* larvae complementary DNA (cDNA) libraries (GenBank Accession Number SRX032364) as well as all expressed sequence tags (ESTs) were downloaded from NCBI (www.ncbi.nlm.nih.gov). All sequences were quality trimmed and *de novo* assembled using CLC Genomics Workbench v3.7 (CLC bio, Katrinebjerg, Denmark). Consensus sequences from short read and EST assemblies were compared to the UniProtKB/Swiss-Prot database (http://www.uniprot.org) using NCBI's BLASTx algorithm (Altschul et al. 1997). Sequences having a top blast hit with an e-

value less that 1E-30 were inspected for genes associated with ceramide metabolism. Individual sequence alignments were performed to determine percent coverage and sequence similarity (Geneious Pro v. 4.8.5; Drummond et al. 2010).

Gene sequencing

Juvenile *C. gigas* (mean length = 11.4 cm) were obtained from Taylor Shellfish Farms, Inc. (Quilcene, WA). Tissues (gill, mantle, adductor muscle, and digestive gland) were dissected from *C. gigas* using sterile techniques and stored in RNAlater (Ambion, Carlsbad, CA). RNA isolation was carried out using Tri-Reagent (Molecular Research Center, Cincinnati, OH) per the manufacturer's protocol. Following RNA isolation, samples were treated with the Turbo DNA-free Kit, rigorous protocol (Ambion) to remove potential genomic DNA carry-over. All samples were evaluated to insure genomic DNA was absent by performing quantitative polymerase chain reaction (qPCR) on DNAsed RNA samples. RNA samples were reverse transcribed using M-MLV reverse transcriptase according to manufacturer's protocol (Promega, Madison, WI).

For genes where the putative open reading frame could be determined based on sequence alignments, PCR primers were designed to amplify entire coding regions (Primer 3 in Geneious Pro v. 4.8.5; Rozen & Akaletsky 2000, Drummond et al. 2010) (Table 1). PCR reactions (25µl) using cDNA from gill tissue were carried out with 12.5 µL 2x Apex RED Taq Master Mix (Genesee Scientific, San Diego, CA), 8.5 µL nuclease-free water, 0.5 µL of 10 µM forward and reverse primers (Integrated DNA Technologies, Coralville, IA), and 3 µL cDNA template. Thermal cycling parameters were as follows: 95°C for 10 minutes; 40 cycles of: 95°C for 30 seconds, 55°C for 30 seconds, and 72°C for 30 seconds; 72°C for 10

minutes. PCR products were separated on agarose gels, checked for expected amplicon size, excised, cloned in pCR 2.1-TOPO Vector, and transformed in to One Shot Top10 chemically competent cells using the TOPO TA Cloning Kit (Invitrogen, San Diego, CA). Plasmid DNA was isolated from bacterial cultures using the Qiagen MiniPrep Kit, following the manufacturer's protocol (Qiagen, Valencia, CA) and sequenced at the High Throughput Genomics Unit (University of Washington) using vector-specific primers (Invitrogen).

Sequences were trimmed to their open reading frame and translated to their amino acid sequences (Geneious Pro v. 4.8.5, Drummond et al. 2010). Sequence alignments were performed using ClustalX v. 2.1 (Larkin et al. 2007).

Protein phylogeny

Using NCBI's HomoloGene database, sequences for corresponding proteins in *Homo sapiens*, *Mus musculus*, *Danio rerio*, *Xenopus tropicalis* and *Caenorhabditis elegans* were downloaded where available. Using the PhyML plugin in Geneious (Guindon & Gascuel 2003; Drummond et al. 2010), maximum likelihood phylogenetic trees of the protein sequences were constructed based on the James-Taylor-Thornton (JTT) model and bootstrapped 100 times (Jones et al. 1992; Guindon & Gascuel 2003).

Quantitative PCR

DNA-free RNA was reverse transcribed to cDNA as described above. qPCR was performed using 1µL of cDNA in a 25µL reaction containing 12.5 µL of 2x Immomix Master Mix (Bioline, London, UK), 0.5 µL of 10 µM forward and reverse primers, 1.0 µL 50µM SYTO13 (Invitrogen), and 9.5 µL nuclease-free water. Primers used for qPCR are listed in

Table 1. Thermal cycling and fluorescence detection was performed using a CFX96 Real-Time Detection System (Bio-Rad, Hercules, CA). Cycling parameters were as follows: 95°C for 10 minutes; 40 cycles of 95°C for 15 seconds, 55°C for 15 seconds, 72°C for 30 seconds. Immediately after cycling, a melting curve protocol was run to verify that a single product was generated in each reaction.

Average Ct (fluorescence-based cycle threshold) values across replicates and average gene efficiencies were calculated with PCR Miner (Zhao & Fernald 2005, http://www.miner.ewindup.info/version2). Gene expression (R_0) was calculated based on the equation $R_0 = 1/(1+E)^{Ct}$, where E is the average gene efficiency and Ct is the cycle threshold for fluorescence. All expression values were normalized to expression of *elongation factor 1α (*GenBank Accession Number AB122066*)*. All qPCRs were run in duplicate and significant differences in expression were determined via pairwise t-tests in R (R Development Core Team 2011) with $\alpha=0.05$.

Bacterial Challenges

For bacterial challenges, *Vibrio vulnificus* was grown in 400 mL culture medium (1x standard Luria-Bertani broth with an additional 1% NaCl) at 37°C for 18 hours at 150 rpm. The culture was then centrifuged for 10 minutes at 4300 rpm (25°C), the supernatant was removed and the pelleted bacteria were resuspended in 50 mL non-sterile of seawater. Eight oysters held in 8 L of seawater were inoculated with *V. vulnificus* at an initial concentration of $4.56x10^{18}$ CFU/L via a 3 hour immersion bath. Control oysters (n=8) were likewise placed in 8L of seawater. Following exposure, oysters were harvested aseptically

and gill tissue was dissected and immediately frozen at -80°C. RNA isolation, reverse transcription and quantitative PCR analysis was carried out as described.

RESULTS

A total of 23 sequences associated with ceramide metabolism were identified by analyzing publicly available *C. gigas* sequences (Table 2). A majority of the genes are either involved in *de novo* synthesis, catabolic generation, or enzymatic breakdown of ceramide (Figure 1). Most sequences were derived from contigs generated by assembling short read sequences (see supplemental data S1). Of the 23 sequences, 4 were selected for further characterization based on the percent of putative open reading frame identified. These four genes include *serine palmitoyltransferase-1* (Cg-*sptlc1)*, *3-ketodihydrosphingosine reductase* (Cg-*3KDSR)*, *acid ceramidase* (Cg-*AC),* and *ceramide glucosyltransferase* (Cg-*GlcCer).* Based on amino acid alignments, complete nucleotide open reading frames were obtained for Cg-*sptlc1* (GenBank Accession Number JN315146), Cg-*3KDSR* (GenBank Accession Number JN315143), and Cg-*AC* (GenBank Accession Number JN315144). Cg-*GlcCer* (GenBank Accession Number JN315145) is missing a portion of the 3' end of the nucleotide sequence as determined from alignments with full-length sequences in other species.

Serine palmitoyltransferase-1

The open reading frame of Cg-*sptlc1* is 1404 bp and is most similar to *sptlc-1* in *Xenopus tropicalis* (GenBank Accession Number NM_001079574) with 71% nucleotide sequence similarity. The next most similar sequence is from the hemichordate,

Saccoglossus kowalevskii (GenBank Accession Number XM_002730516, with 70% identity). At the amino acid level Cg-*sptlc1* is most similar to serine palmitoyltransferase 1 in the Sumatran orangutan, *Pongo abelii* (GenBank Accession Number Q5R9T5). Based on alignments at the deduced amino acid level, Cg-*sptlc1* shares 59.8% pairwise identity with the *H. sapiens* homolog and 51.0% pairwise identity over 475 amino acids with *C. elegans* Sptlc1 (Figure 2).

The highest level of Cg-*sptlc1* gene expression was detected in gill tissue, followed by digestive gland, mantle, and then adductor muscle (data not shown). Expression levels in gill tissue were 40 times higher the levels in adductor muscle tissue. Cg-*sptlc1* expression was not significantly altered in gill tissue from oysters exposed to *Vibrio*, compared to controls. ($p=0.068$; Figure 6).

3-ketodihydrosphingosine reductase

The Cg-*3KDSR* open reading frame is 1129 bp and is most similar to the *Rattus norvegicus 3KDSR* sequence (GenBank Accession Number NM_001108342) with a sequence identity of 68%. The second most similar sequence is *3KDSR* from *Saccoglossus kowalevskii* (GenBank Accession Number SM_002740331, 76%). The amino acid translation of Cg-*3KDSR* is most similar to *M. musculus* 3KDSR (GenBank Accession Number Q6GV12). The *C. gigas* amino acid sequence shares 50.8% identity to the corresponding homolog in *H. sapiens* (Figure 3). Based on the derived amino acid sequence of Cg-*3KDSR,* the catalytic site and NADH/NADPH binding site (Kihara & Igarashi 2004) are conserved in oysters (Figure 3). Gene expression of Cg-*3KDSR* was highest in gill tissue with expression levels over 1000 times higher compared to other tissues (data not shown). Cg-*3KDSR* gene

204 expression in *Vibrio*-exposed oysters was not different from controls (p=0.079; Figure 6).

205

206 *Ceramide glucosyltransferase*

207 Cg-GlcCer (1124bp) is most similar to ceramide glucosyltransferase from the human
208 body louse, *Pediculus humanus corporis* (GenBank Accession Number SM_002431306,
209 sequence similarity of 66%), followed by *Xenopus laevis* UDP-glucose ceramide
210 glucosyltransferase (GenBank Accession Number NM_001090475, sequence similarity of
211 66%). The translated amino acid sequence is most similar to *Xenopus tropicalis* ceramide
212 glucosyltransferase (GenBank Accession Number Q5BL38). *C. gigas* and *H. sapiens* share a
213 45.9% pairwise amino acid identity over 396 residues in the alignment, while *C. elegans*
214 and *C. gigas* share 40.9% pairwise identity over 468 residues (Figure 4).

215 Cg-*GlcCer* had a similar expression profile across tissues to Cg-*sptlc1*, the highest
216 expression being in the gill, followed by digestive gland, mantle and adductor (data not
217 shown). The Cg-*GlcCer* gene was not expressed differently in *Vibrio*-exposed oysters
218 compared to control oysters (p=0.47; Figure 6).

219

220 *Acid ceramidase*

221 The open reading frame for Cg-*AC* is 1170 bp in length and was most similar to the
222 gene BRF 7-G7 in *Sebastes schlegelii* (Schlegel's black rockfish, GenBank Accession Number
223 AB491143), with a sequence similarity of 67%. The translated amino acid sequence for *C.*
224 *gigas* is the most similar to *Rattus norvegicus* acid ceramidase (GenBank Accession Number
225 Q6P71). The Cg-*AC* amino acid sequence shares 46.6% pairwise identity over 402 residues
226 in the alignment with *C. elegans* and 49.4% identity with the *H. sapiens* sequence over 398

227 residues (Figure 5).

228 Cg-*AC* was expressed the most in the gill tissue followed by digestive gland, mantle,
229 and adductor (data not shown). The expression of Cg-*AC* was significantly higher in *Vibrio*-
230 exposed oysters compared to controls (p=0.045; Figure 6).

231

232 All four genes showed similar phylogenetic topologies (Figure 7), with the amino
233 acid sequences clustering into distinct invertebrate and vertebrate lineages. When the *C.*
234 *elegans* sequence was available and included in the phylogeny, it clustered with the *C. gigas*
235 sequence with a bootstrap value of 100%. *H. sapiens* and *M. musculus* sequences always
236 clustered together with a bootstrap of 100%.

237

238 DISCUSSION

239 This study identified a suite of genes associated with ceramide metabolism in the
240 Pacific oyster, including the direct sequencing and characterization of *serine*
241 *palmitoyltransferase-1* (Cg-*sptlc1*), *acid ceramidase* (Cg-*AC*), *3-ketodihydrosphingosine*
242 *reductase* (Cg-*3KDSR*), and *ceramide glucosyltransferase* (Cg-*GlcCer*). These data provide an
243 important resource for further studies that focus on the role of ceramide in the
244 environmental response in invertebrates. While well studied in vertebrate systems, there
245 have been only a few recent studies that focus on ceramide metabolism and signaling in
246 molluscs (see Lee et al. 2011; Zhang et al. 2011; Romero et al. 2011).

247 Numerous genes associated with ceramide metabolism are conserved across distant
248 taxonomic lineages. In vertebrates, the genes described here are directly responsible for
249 synthesis of ceramide (*sptlc1, 3KDSR*; Figure 1) and generation of sphingolipids from

ceramide (*AC* and *GlcCer*). *In silico* analysis of the *C. gigas* transcriptome shows that there are a number of other genes in these ceramide metabolism pathways (Table 2). In fact, almost all the genes coding for enzymes necessary for *de novo* ceramide synthesis were identified, suggesting a conservation of this metabolic pathway in *C. gigas*. Additionally, a number of enzymes responsible for transformation of ceramide into other lipid products were identified including ceramide kinase, ceramide synthase , and sphingomyelin synthase . A variety of caspases, TNF superfamily receptors, RIP (receptor-interacting serine/threonine-protein) and FADD (Fas-associated protein with death domain) subunits of the TNFα (tumor necrosis factor) receptor, which are key components of the cellular stress and apoptotic responses, were also identified in public databases . Several genes known to be involved in ceramide metabolism were not found in this effort (i.e. dihydroceramide desaturase, ceramide-1P phosphatase). This is likely related to the fact that these genes have yet to be sequenced in the Pacific oyster. It is also possible that corresponding enzymes lack significant sequence homology. Once a complete genome is sequenced for this species, a more comprehensive analysis could be performed.

Sptlc1, responsible for accumulation of intracellular ceramide during cellular stress (Perry et al. 2000; Perry 2002), is highly conserved in oysters including a 21 residue transmembrane region originally identified in *H. sapiens* (Handa 2003). The serine palmitoyltransferase identified in *C. gigas* has high homology with the LCB1 *H. sapiens* isoform. There are two forms of *H. sapiens* Sptlc – LCB1 and LCB2 (Hanada 2003). *H. sapiens* LCB2 has a conserved motif that binds pyridoxal phosphate (PLP) (Hanada 2003; Momany et al. 2008), but LCB1 has an asparagine instead, which is homologous to the *C.*

gigas sequence. In *H. sapiens*, LCB1 is necessary for the maintenance of LCB2 and does not perform the same catalytic functions (Hanada 2003). More research is needed to determine if the functionality of specific Sptlc isoforms are conserved across taxa.

C. gigas 3KDSR shares conserved catalytic domains with all other amino acid sequences in the alignment, suggesting that its functionality is conserved across taxonomic groups. 3-ketodihydrosphingosine reductase acts downstream of Sptlc. The product of the reaction catalyzed by Sptlc is 3-ketosphinganine. 3-ketosphinganine is reduced by a NADPH-dependent reductase to dihydrosphingosine. The enzyme that catalyzes this reaction is 3-ketodihydrosphingonsine reductase (3KDSR). 3KDSR contains two functional sites that are highly conserved, based on the amino acid alignment: an NADH/NADPH binding site and a catalytic site (Kihara & Igarashi 2004; Figure 3). All four amino acid sequences – *C. gigas*, *H. sapiens*, *M. musculus*, and *D. rerio* - share more of the catalytic site motif than previously described: *Tyr-Ser-X-Ser-Lys*, beginning at position 187 on the alignment (Kihara & Igarashi 2004; Figure 3). The motif of the NADH/NADPH binding site is identical in its entirety – *Gly-Gly-Ser-Ser-Gly-Ile-Gly* – across all four sequences/taxa (Kihara & Igarashi 2004; Figure 3).

The gene expression patterns observed for each gene are consistent with a role of ceramide metabolism in the stress response. The highest expression was observed in the gill tissue, which is rich with hemocytes, the primary immune cell in bivalves. Furthermore, exposure to *V. vulnificus* significantly elevated expression of Cg-*AC*. There are several possible interpretations of this increase in gene expression that corroborate with the

second messenger role of ceramide. For instance, increased expression of Cg-*AC* could indicate that ceramide is transformed into the lipid sphingosine, which then functions downstream as a signaling molecule in the *C. gigas* immune response. Sphingosine is an important signaling molecule in the vertebrate immune response and probably plays a similar role in invertebrates. Sphingosine is associated with the inhibition of the proliferation of Th2 T cells, inhibition of protein kinase C activity, regulation of the complement system, and inhibition of neutrophil respiratory burst (Merrill & Stevens 1989; Baumruker & Prieschl 2002). The roles that sphingosine and other sphingolipids play in the immune response seem to be heavily influenced by their concentrations (Baumruker & Prieschl 2002), thus Cg-*AC* could be a pivotal enzyme regulating levels of sphingosine in oyster.

An alternative explanation for the increased expression of Cg-*AC* during *V. vulnifcus* challenge suggests that ceramide is the primary signaling molecule in the *C. gigas* immune response. An accumulation of ceramide in response to the *V. vulnificus* exposure could have occurred and Cg-*AC* may be up-regulated to metabolize ceramide after it has performed its signaling roles. Ceramide may have been produced to increase signaling of immune pathways necessary for responding to bacterial exposure. Increased expression of AC has been shown to decrease intracellular ceramide in mammals (Strelow et al. 2000; Chavez et al. 2005) and could very well play the same role in invertebrates. In support of this second hypothesis, the genes Cg-*sptlc1* and Cg-*3KDSR,* responsible for the synthesis of ceramide, showed trends towards up-regulation after *V. vulnificus* exposure, although the differences in expression were not significant.

Here we report the identification of numerous genes in *C. gigas* involved in the

metabolism of ceramide, an important lipid signaling molecule. Gene expression analysis suggests that ceramide is involved in the immune response of oysters exposed to microbial pathogens. It should be noted that a limited number of genes were examined here and targeted studies would be required to further elucidate the functional role of ceramide metabolism in bivalves. For instance future efforts might directly quantify sphingolipid levels and correlate levels with specific cellular function. Furthermore, it is not known if lipid content in bivalve diets impacts stress physiology by influencing ceramide levels. Characterizing how diet and other conditions affect ceramide metabolism could offer a framework for better understanding mechanisms associated environmental effects on immune function.

ACKNOWLEDGEMENTS

We thank Sam White for his help with the lab work that was part of this study. We would also like to thank Taylor Shellfish, Inc. for their generous donation of oysters. Thank you to Mackenzie Gavery, Lisa Crosson, Dave Metzger, and Sam White for their critical review of this manuscript. This research was funded in part by the National Oceanographic and Atmospheric Administrations Saltonstall-Kennedy Grant and in part by the University of Washington's School of Aquatic and Fishery Sciences.

REFERENCES

Altschul, S.F., Madden, T.L., Schaeffer, A.A., Zhang, J., Zhang, Z., Miller, W., Lipman, D.J., 1997. Gapped BLAST and PSI-BLAST: a new generation of protein database search programs, Nucleic Acids Res. 25, 3389-3402.

342

343 Ballou, L.R., Chao, C.P., Holness, M.A., Barker, S.C., Raghow, R., 1992. Interleukin-1-
344 mediated PGE2 production and sphingomyelin metabolism. Evidence for the regulation of
345 cyclooxygenase gene expression by sphingosine and ceramide. The Journal of Biological
346 Chemistry 267, 20044-20050.

347

348 Ballou, L.R., Laulederkind, S.J., Rosloniec, E.F., Raghow, R., 1996. Ceramide signaling and the
349 immune response. Biochimica et Biophysica Acta 1301, 273-287.

350

351 Baumruker, T., Prieschl, E.E., 2002. Sphingolipids and the regulation of the immune
352 response. Semin. Immunol. 14, 57-63.

353

354 Chavez, J.A., Holland, W.L., Bär, J., Sandhoff, K., Summers, S.A., 2005. Acid ceramidase
355 overexpression prevents the inhibitory effects of saturated fatty acids on insulin signaling.
356 The Journal of Biological Chemistry 280, 20148-20153.

357

358 Drummond, A.J., Ashton, B., Buxton, S., Cheung, M., Cooper, A., Heled, J., Kearse, M., Moire, R.,
359 Stones-Havas, S., Sturrock, S., Thierer, T., Wilson, A., 2010. Geneious v4.5.6. Available from
360 http://www.geneious.com

361

362 El Babili, M., Brichon, G., Zwingelstein, G., 1996. Sphingomyelin metabolism is linked to salt
363 transport in the gills of euryhaline fish. Chemistry and Materials Science. 31: 385-392.

364

365 Eliyahu, E., Park, J.-H., Shtraizent, N., He, X., Schuchman, E.H., 2007. Acid ceramidase is a
366 novel factor required for early embryo survival. FASEB J. 21, 1403-1409.
367
368 Guindon, S., Gascuel, O., 2003. A simple, fast, and accurate algorithm to estimate large
369 phylogenies by maximum likelihood. Syst. Biol. 52, 696-704.
370
371 Hanada, K., 2003. Serine palmitoyltransferase, a key enzyme of sphingolipid metabolism.
372 Biochimica et Biophysica Acta – Molecular and Cell Biology of Lipids. 1632, 16-30.
373
374 Hannun, YA., 1994. The sphingomyelin cycle and the second messenger function of
375 ceramide. The Journal of Biochemical Chemistry. 269, 3125-3128.
376
377 Hannun, Y.A., Luberto, C., 2000 Ceramide in the eukaryotic stress response. Trends in Cell
378 Biology. 10, 73-80.
379
380 Jones, D.T., Taylor, W.R., Thornton, J.M., 1992. The rapid generation of mutation data
381 matrices from protein sequences. Comput Appl Biosci. 8, 275-282.
382
383 Kihara, A., Igarashi, Y., 2004. FVT-1 is a mammalian 3-Ketodihydrosphingosine Reductase
384 with an active site that faces the cytosolic side of the endoplasmic reticulum membrane.
385 The Journal of Biological Chemistry 279, 49243-49250.
386

Larkin, M.A., Blackshields, G., Brown, N.P., Chenna, R., McGettigan, P.A., McWilliam, H., Valentin, F., Wallace, I.M., Wilm, A., Lopez, R., Thompson, J.D., Gibson, T.J., Higgins, D.F., 2007. Clustal W and Clustal X version 2.0. Bioinformatics 23, 2947-2948.

Lee, Y., De Zoysa, M., Whang, I., Lee, S., Kim, Y., Oh, C., Choi, C.Y., Yeo, S.-Y., Lee, J., 2011. Molluscan death effector domain (DED)-containing caspase-8 gene from disk abalone (*Haliotis discus discus*): Molecular characterization and expression analysis. Fish & Shellfish Immunology 30, 480-487.

Merrill Jr, A.H., Stevens, V.L., 1989. Modulation of protein kinase C and diverse cell functions by sphingosine – a pharmacologically interesting compound linking sphingolipids and signal transduction. Biochimica et Biophysica Acta 1010, 131-139.

Momany, C., Ghosh, R., Hackert, M.L., 2008. Structural motifs for pyridoxal-5'-phosphate binding in decarboxylases: An analysis based on the crystal structure of the *Lactobacillus* 30a ornithine decarboxylase. Protein Sci. 4, 849-854.

Perry, D.K., 2002. Serine palmitoyltransferase: role in apoptotic de novo ceramide synthesis and other stress responses. Biochimica et Biophysica Acta – Molecular and Cell Biology of Lipids 1585, 146-152.

Perry, D.K., Bielawska, A., Hannun, Y.A., 2000. Quantitative determination of ceramide using diglyceride kinase. Methods Enzymol. 312, 22-31.

R Development Core Team. 2011. R: A language and environment for statistical computing. R Foundation for Statistical Computing. Vienna, Austria. www.R-project.org.

Romero, A., Estévez-Calvar, N., Dios, S., Figueras, A., Novoa, B., 2011. New insights into the apoptotic process in mollusks: characterization of caspase genes in *Mytilus galloprovincialis*. PLoS ONE. 6:e17003. doi:10.1371/journal.pone.0017003.

Rozen, S., Skaletsky, H.J., 2000. Primer3 on the WWW for general users and for biologist programmers. In: Krawetz, S., Misener, S. (Eds) Bioinformatics Methods and Protocols: Methods in Molecular Biology, Humana Press, Totowa, NJ, pp. 365-386.

Strelow, A., Bernardo, K., Adam-Klages, S., Linke, T., Sandhoff, K., Krönke, M., Adam, D., 2000. Overexpression of acid ceramidase protects from tumor necrosis factor-induced cell death. The Journal of Experimental Medicine 192, 601-612.

Verheij, M., Bose, R., Lin, X.H., Yao, B., Jarvis, W.D., Grant, S., Birrer, M.F., Szabo, E., Zon, L.I., Kyriakis, J.M., Haimovitz-Friedman, A., Fuks, Z., Kolesnick, R.N., 1996. Requirement for ceramide-initiated SAPK/JNK signaling in stress-induced apoptosis. Letters to Nature 380, 75-79.

Zhang, L., Li, L., Zhang, G., 2011. Gene discovery, comparative analysis and expression profile reveal the complexity of the *Crassostrea gigas* apoptosis system. Dev. Comp. Immunol. 35, 603-610.

Zhao, S., Fernald, R.D., 2005. Comprehensive algorithm for quantitative real-time polymerase chain reaction. Comput. Biol. 12, 1045-1062.

FIGURE CAPTIONS

Table 1. Sequencing and qPCR primer sequences.

Table 2. Genes associate with ceramide metabolism were identified in *C. gigas* by searching of publicly available databases. Sequences assembled from short read archive data and expressed sequence tags were given a Gene ID code that corresponds to the sequence in the supplementary information (S1). For each of these contiguous sequences, the top BLASTx hit description, corresponding species, and e-value are provided. Two genes that were identified as a single EST (sphingomyelin synthase and ceramide synthase) are denoted with their respective GenBank Accession Numbers. An additional four genes (GenBank Accession Numbers HQ425699, HQ425701, HQ425703, and HQ425705) have been previously characterized in *C. gigas* (Zhang et al. 2011).

Fig. 1. Representation of the major players in the ceramide metabolism pathways. Enzymes are in white italics with the genes characterized as part of this study in bold: *serine palmitoyltransferase*, *3-ketodihydrosphingosine reductase*, *ceramide glucosyltransferase*, and *acid ceramidase*. Compounds that are either precursors, or the products of enzymatic break-down of ceramide, are shown in black. The pathway is adapted from Ballou et al. (1996) and Hannun and Luberto (2000).

Figure 2. Amino acid alignment of translated Cg-*sptlc1* with protein sequence of *C. elegans* (GenBankAccession Number NP_001021978), *H. sapiens* (GenBank Accession Number NP_006406), *M. musculus* (GenBank Accession Number NP_033295), and *D. rerio* (GenBank Accession Number NP_001018307). Black shading indicates 100% similarity across sequences, dark gray is 80-100% similarity, light gray is 60-80% similarity, and white is less than 60% similarity. The transmembrane domain is marked by the dashed box and the

476 asparagine that corresponds to the *H. sapiens* LCB1 isoform is marked with an arrow.

477

478 Figure 3. Amino acid alignment of translated Cg-*3KDSR* with protein sequence from *H.*
479 *sapiens* (GenBank Accession Number Q06136), *M. musculus* (GenBank Accession Number
480 NP_081810), and *D. rerio* (GenBank Accession Number NP_957433). Black shading
481 indicates 100% similarity across sequences, dark gray is 80-100% similarity, light gray is
482 60-80% similarity, and white is less than 60% similarity. The conserved catalytic site is
483 marked with an asterisk and the NADH/NADPH binding site and active site motif is marked
484 with a diamond.

485

486 Figure 4. Amino acid alignment of translated Cg-*GlcCer* with ceramide glucosyltransferase
487 protein sequences from *C. elegans* (GenBank Accession Number NP_506971), *H. sapiens*
488 (GenBank Accession Number NP_003349), *M. musculus* (GenBank Accession Number
489 NP_035803), and *X. tropicalis* (GenBank Accession Number Q5BL38). Black shading
490 indicates 100% similarity across sequences, dark gray is 80-100% similarity, light gray is
491 60-80% similarity, and white is less than 60% similarity.

492

493 Figure 5. Amino acid alignment of translated Cg-*AC* with protein sequences from acid
494 ceramidase in *C. elegans* (GenBank Accession Number NP_493173), *H. sapiens* (GenBank
495 Accession Number NP_808592), *M. musculus* (GenBank Accession Number NP_062708),
496 and *D. rerio* (GenBank Accession Number NP_001006088). Black shading indicates 100%
497 similarity across sequences, dark gray is 80-100% similarity, light gray is 60-80%
498 similarity, and white is less than 60% similarity.

Figure 6. Expression values in gill tissue for *serine palmitoyltransferase-1* (Cg-*sptlc1*), *3-ketodihydrosphingosine reductase* (Cg-*3KDSR*), *glucosylceramidase* (Cg-*GlcCer*), and *acid ceramidase* (Cg-*AC*) . Gene expression values for the control ("C") oysters are represented by the gray boxes, while the *V. vulnificus*-exposed ("Vv") oysters are represented with the white boxes. Boxes represent the spread of the middle 50% of the data with the median shown as the horizontal black line in the box. The dotted lines span the remaining data. An asterisk indicates a significant difference in expression between exposed and control oysters.

Figure 7. Maximum likelihood phylogenetic tree of the amino acid alignment of acid ceramidase in *C. gigas*, *C. elegans*, *H. sapiens*, *M. musculus*, and *D. rerio*. All other protein trees had similar topology to the one shown. The tree was created based on the James-Taylor-Thornton (JTT) model and bootstrapped 100 times.

TABLES

516

517 Table 1

Gene	Description	Sequencing Forward Primer	Sequencing Reverse Primer	Sequence Product Size (bp)	qPCR Forward Primer	qPCR Reverse Primer	qPCR Product Size (bp)
EF1α	elongation factor 1α	-	-	-	CAGCACAGTCAGCCTGTGAAGT	AAGGAAGCTGCTGAGATGGG	200
Sptlc1	serine palmitoyltransferase	ATGGCGTCGACGTTCATTCC	CTGTTCCCCAATATTTCTGAC	1483	TTCACAGCAAGCTGAGCGAT	AAGTAGCGAGCCAACGTCAC	178
3KDSR	3-ketodihydrosphingosine reductase	AGCGACGGACCGAACTTACT	TGTCTTGGGTTTTGCATCCTTC	1210	GCAGTGCAGTGGCTGGAAAT	AGGCAGCCTTGGTGACATTG	168
AC	acid ceramidase	TGTGATTACACGATGTGGATACCG	CTGCTTCTGACTTCCGGTGT	1165	TGGACTCAAGTTGGCCAGGA	AAGGCTGGGGGAGAGTATCG	157
GlcCer	glucosylceramide synthase	AGAGGCGAACACACGAAAGT	CCATATGGATAACACTTCTCG	1080	TTGGCCCAAACGGGAAAGTT	TGTCCATGAGCGAGTCTGGT	114

Gene ID	Gene Description	Species	e-value
Cg_4852	Serine palmitoyltransferase-1	*Pongo abelii*	0.00E+00
Cg_877	Acid ceramidase	*Rattus norvegicus*	2.00E-146
Cg_14141	3-ketodihydrosphingosine reductase	*Mus musculus*	1.00E-122
Cg_29918	Ceramide glucosyltransferase	*Xenopus tropicalis*	9.00E-122
Cg_21728	Acid sphingomyelinase	*Mus musculus*	5.00E-46
Cg_16356	Ceramide kinase	*Homo sapiens*	1.00E-27
Cg_16726	Cerebrosidase	*Mus musculus*	5.00E-139
Cg_17230	Neutral ceramidase	*Oryza sativa*	5.00E-96
Cg_1560	Caspase 7	*Homo sapiens*	4.00E-10
Cg_23531	Caspase 8	*Homo sapiens*	8.00E-54
Cg_252	TNF receptor-associated factor 2	*Mus musculus*	1.00E-53
Cg_3248	TNF receptor-associated factor 3	*Mus musculus*	2.00E-30
Cg_31180	TNF receptor-associated factor 4	*Homo sapiens*	4.00E-39
Cg_6808	Neutral Sphingomyelinase	*Caenorhabditis elegans*	4.00E-10
Cg_20643	Dihydrosphingosine 1-phosphate phosphatase	*Schizosaccharomyces pombe*	3.00E-09
Cg_26221	Sphingosine-1-phosphate phosphatase	*Mus musculus*	8.00E-20
Cg_7888	Sphingosine-1-phosphate lyase	*Dictyostelium discoideum*	6.00E-09
HS213433	Sphingomyelin synthase	*Homo sapiens*	1.00E-100
HS185280	Ceramide synthase	*Mus musculus*	5.00E-83
HQ425699	Fas-associated receptor with Death Domain	*Crassostrea gigas*	-
HQ425701	Inhibitor of apoptosis	*Crassostrea gigas*	-
HQ425703	Caspase 1	*Crassostrea gigas*	-
HQ425705	Caspase 2	*Crassostrea gigas*	-

Table 2

FIGURES

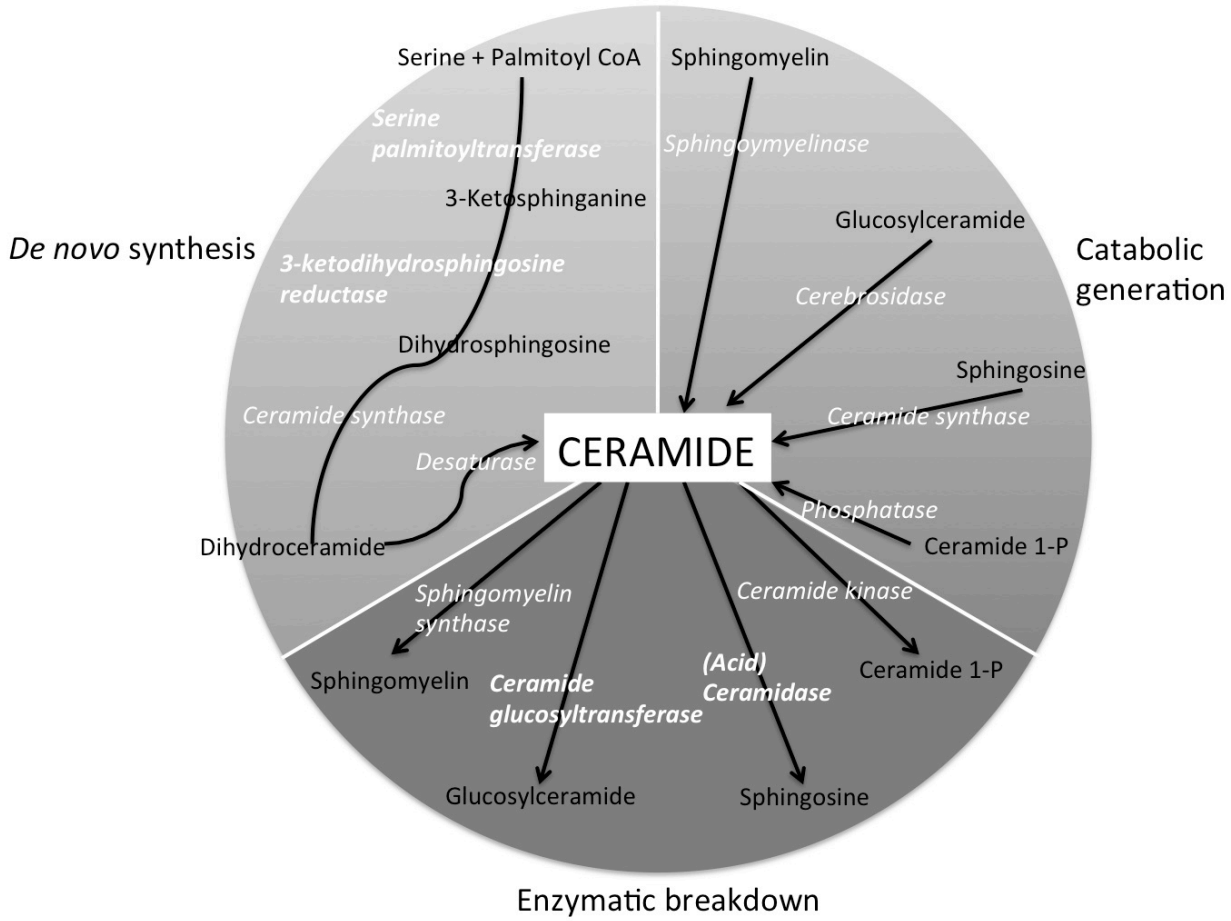

532

533

534 Figure 1

535

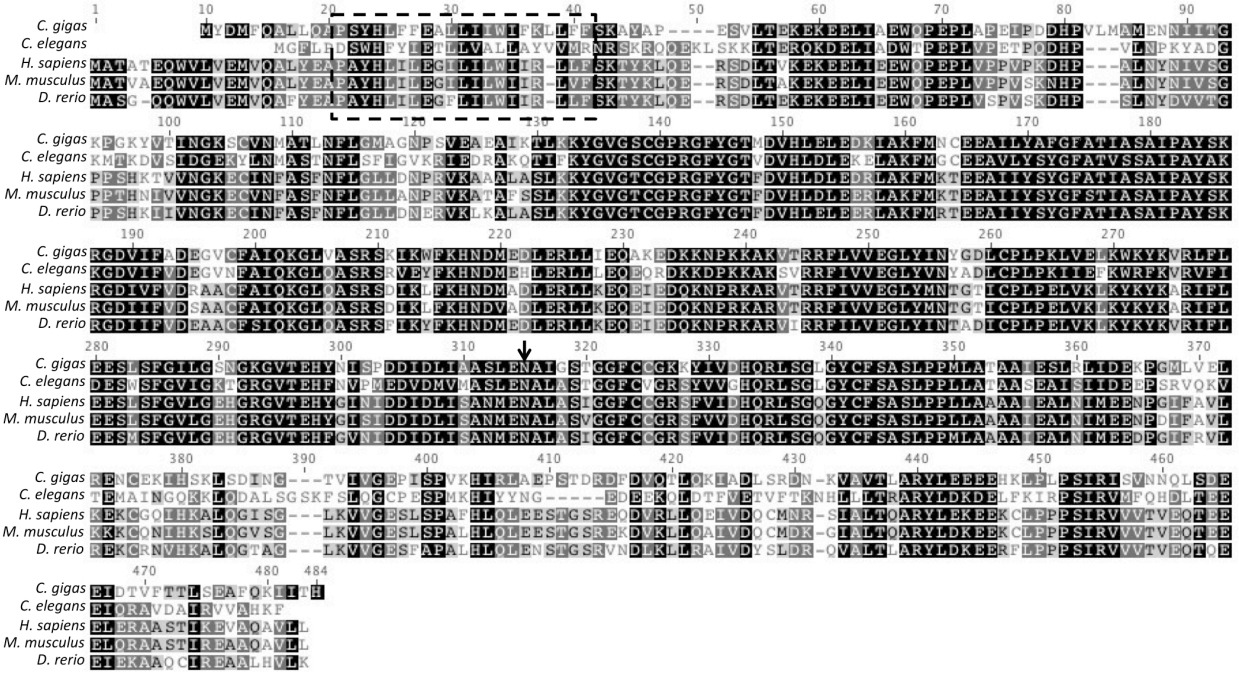

536

537 Figure 2

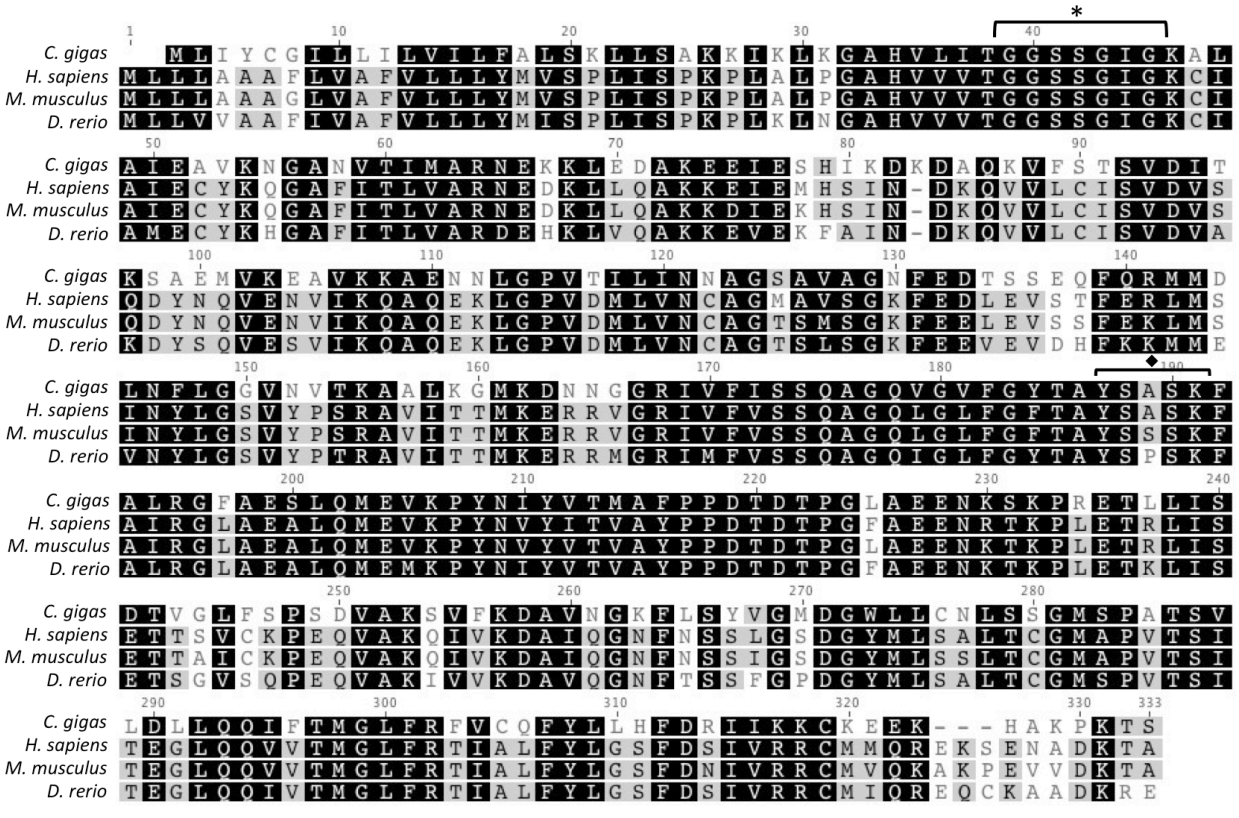

538

539 Figure 3

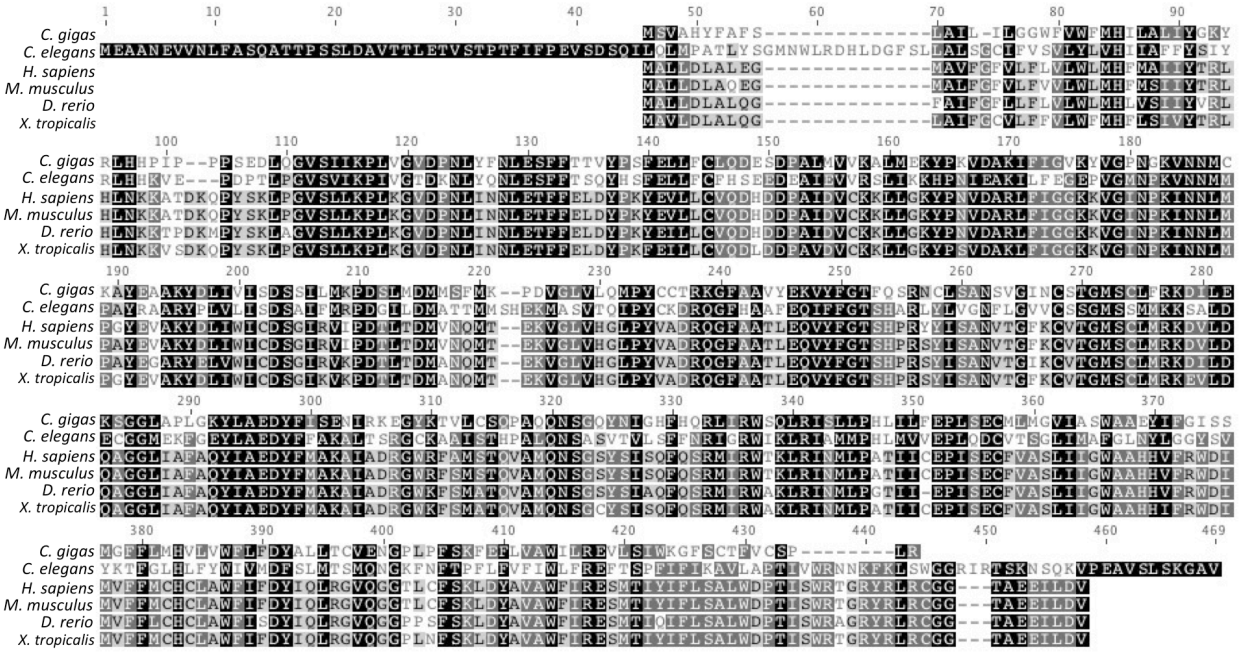

Figure 4

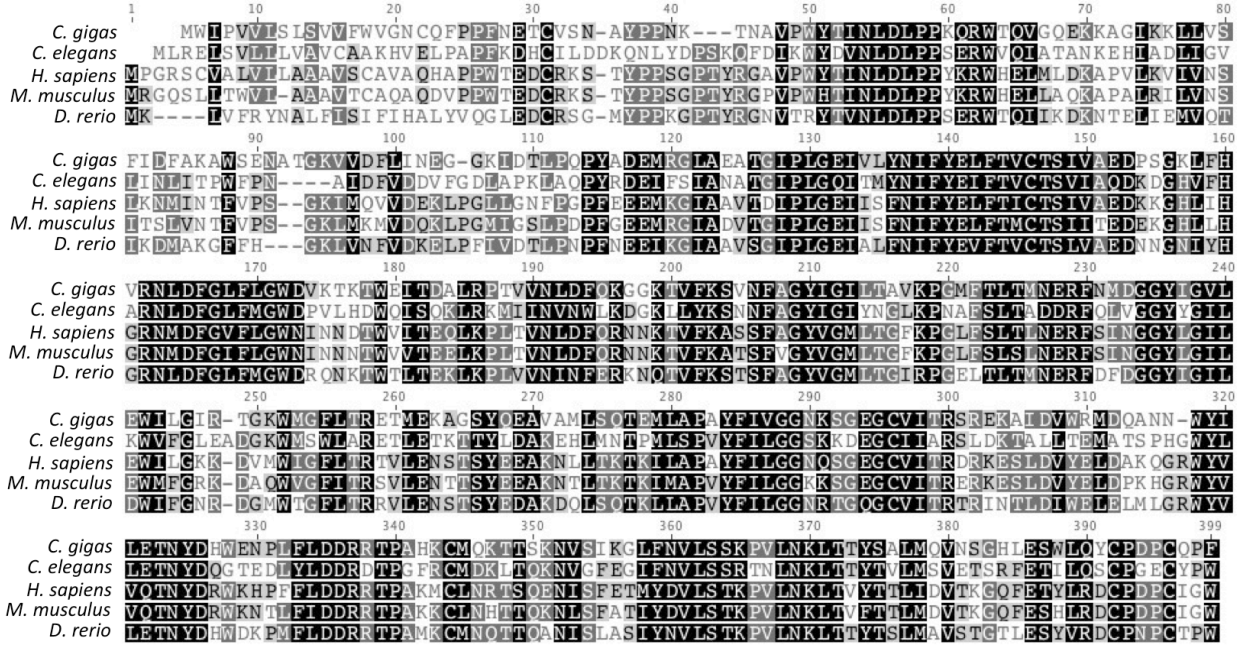

Figure 5

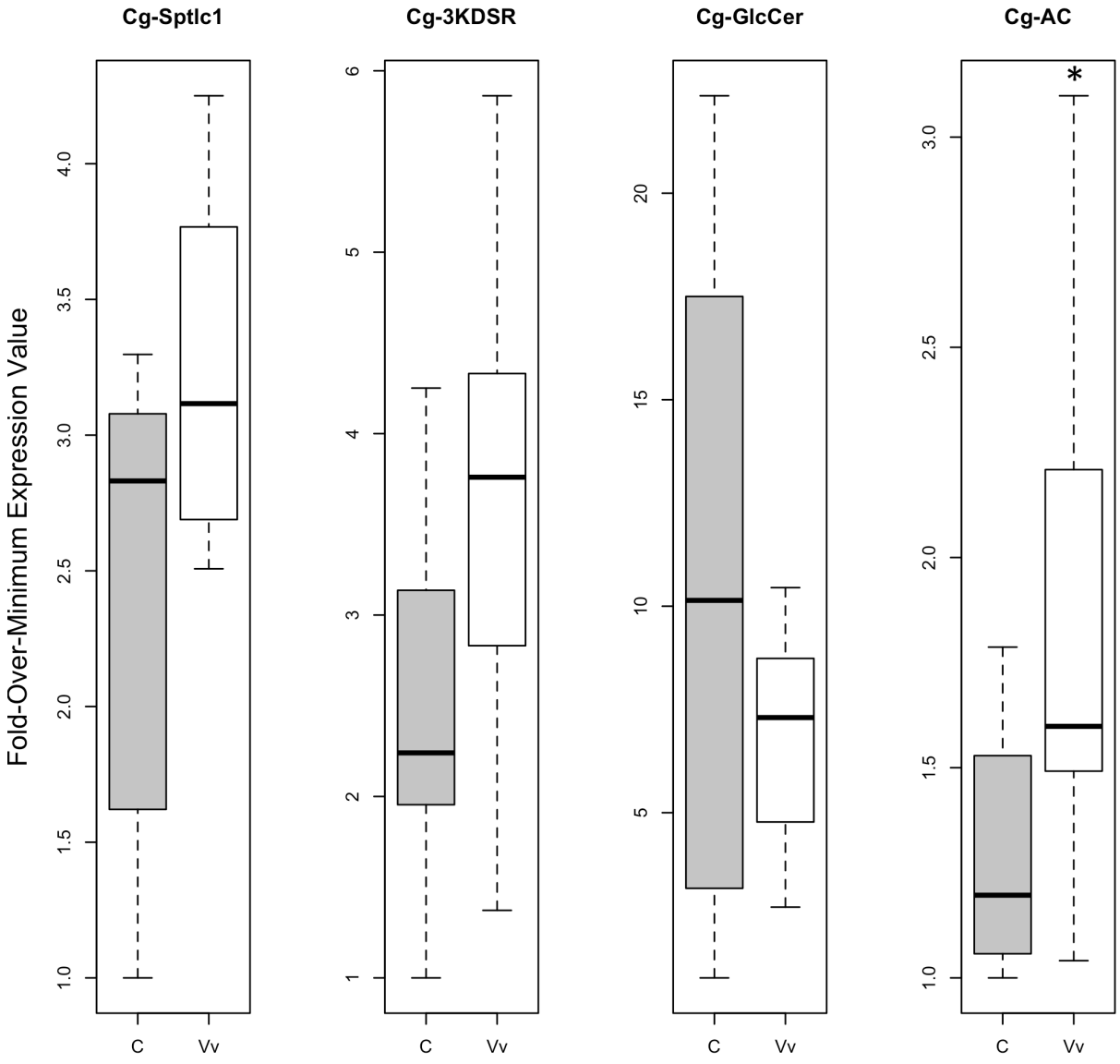

544

545 Figure 6

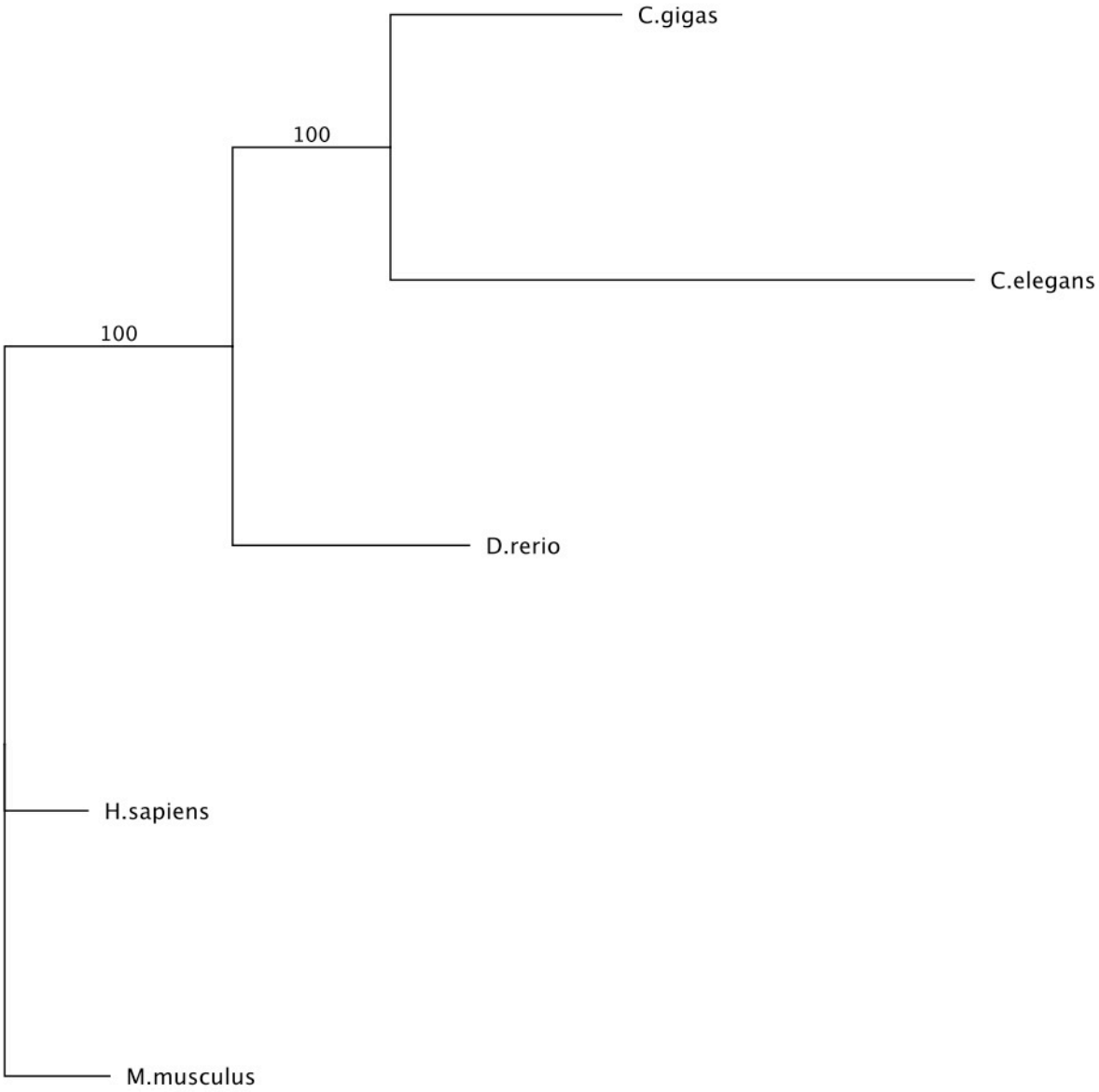

546

547 Figure 7